

# Molecular motion in concentrated solutions of spherical polystyrene microgels studied with the pulsed field gradient n.m.r.

Gerald Fleischer\*

Abt. Polymerphysik, Fachbereich Physik, Universität Leipzig, Linnéstrasse 5, D-04103 Leipzig, Germany

and Hans Sillescu

Institut für Physikalische Chemie, Universität Mainz, Jakob-Welder-Weg 15, D-55099 Mainz, Germany

and Vladimir D. Skirda

Physics Department, Kazan State University, Lenina 18, 430008 Kazan, Tatarstan, Russia  
(Received 21 June 1993; revised 22 October 1993)

Results of a pulsed field gradient n.m.r. study of the motion of swollen spherical microgels in solution are presented. We have measured the echo attenuation (or the incoherent dynamic structure function) of the protons in the microgels in the dynamic range from  $qR \ll 1$  up to  $qR \approx 1.8$  (where  $q$  = scattering vector and  $R$  = particle radius), and in the timescale from a few milliseconds up to 100 ms. Rotational diffusion of the microgel spheres could not be detected with certainty. However, restricted diffusion of the spheres within a cage was observed, in particular for the large microgel with  $R = 125$  nm, where the short-time diffusion could be monitored. For apparent volume fractions  $\Phi > 0.6$ , the diffusion is restricted within a space scale of root mean square displacement,  $\langle z^2 \rangle^{1/2} \approx 120$  nm. With increasing volume fraction of the microgels in solution,  $\Phi > 0.6$ , the diffusion becomes increasingly restricted. This crossover corresponds to the dynamic glass transition observed by Bartsch *et al.* for a similar system using quasielastic light scattering.

(Keywords: polystyrene microgels; concentrated solutions; self-diffusion)

## INTRODUCTION

The pulsed field gradient nuclear magnetic resonance (p.f.g. n.m.r.) technique is widely used for observation of the long-range dynamics of molecular systems<sup>1,2</sup>. P.f.g. n.m.r. is a generalized incoherent quasielastic scattering experiment; the measured quantity is the incoherent intermediate structure function  $S(q, t)$  of the protons in the system<sup>3</sup>, commonly called echo attenuation and denoted by  $\Psi$  or  $E_q$ . The generalized scattering vector  $q$  of p.f.g. n.m.r. is given by  $q = \gamma \delta g$ , where  $\gamma$  is the gyromagnetic ratio of the proton,  $\delta$  the width and  $g$  the magnitude of the field gradient pulses. In a typical p.f.g. n.m.r. experiment  $1/q$  is in the order of  $1 \mu\text{m}$ , i.e. in homogeneous non-structured systems we measure in the diffusion limit and obtain the self-diffusion coefficients of the species in the system. However, with p.f.g. n.m.r. the observation of more complicated modes of motion and structures is possible, which in molecular systems mostly appear in space scales smaller than the micrometre region. Examples are the dynamics of polymer molecules and molecules in micellar solutions and porous systems. For this purpose it is necessary to increase the field gradient

intensity and hence  $q$ . At present, pulsed field gradients of about  $50 \text{ T m}^{-1}$  are applied and values of  $1/q < 100 \text{ nm}$  are reached<sup>4-6</sup>. A very promising development is n.m.r. in the stray field of a cryomagnet<sup>7,8</sup>.

The motion of sterically stabilized spherical particles in solution has been studied intensively<sup>9,10</sup>. These particles show interesting features: different dynamic ranges of short-time and long-time diffusion, hydrodynamic interaction and direct hard-core interaction. The motion of these particles is also a matter of intense theoretical investigation. Quasielastic light scattering is a very convenient method to study these systems experimentally, preferentially in dilute solution under the condition  $qR \ll 1$ , where  $R$  is the particle radius. For large particles  $qR \geq 1$  can be reached, and in dense systems the short-time diffusion can be detected in the experiment<sup>9-11</sup>.

Antonietti and co-workers<sup>12,13</sup> have synthesized spherical crosslinked polystyrene beads; these beads swell in solution behaving like 'rubber balls', and no sterical stabilization is necessary. A p.f.g. n.m.r. study of these spherical particles in solution is possible since the nuclear magnetic relaxation times of the swollen network chains are long enough to provide a spin echo in the n.m.r. experiment. For solid latex spheres the short nuclear magnetic relaxation times prevent an n.m.r. signal in the

\* To whom correspondence should be addressed

timescale of p.f.g. n.m.r. The microgels can be prepared with a hydrodynamic radius in benzene or toluene of more than 100 nm, therefore with high field gradients we reach the dynamic range of  $qR > 1$ . We have, at least in principle, the possibility to monitor rotational diffusion of particles with p.f.g. n.m.r. which, to our knowledge, has not been reported to date.

The motion of the microgels is different from the motion of linear chains in solution: the microgels must be considered as semirigid inside, and they cannot interpenetrate. There is no crossover from dilute to semidilute solution at a well defined overlap concentration  $c^*$ . However, at high concentration we approach a dense packing of spheres in the solution. This is connected with a colloidal glass transition<sup>14</sup>.

In this paper we report the first results from the study of diffusive motion of spherical microgels in solution with p.f.g. n.m.r.

## EXPERIMENTAL

### Microgels

The microgels were synthesized and characterized as described in refs 12 and 13. We have investigated a fairly large microgel and, for comparison, two smaller, less well characterized microgels. The characteristic data are given in Table 1.

The solutions were prepared directly in n.m.r. sample tubes with an outer diameter of 7.5 mm. The inner glass surface was treated with trichlorooctadecylsilane to prevent adsorption of the microgels at the glass walls. Deuterated benzene and toluene were used as solvents. No differences were observed in the results from these two solvents. The concentrations are given as mass percentage of polymer,  $c$ , and as the volume fraction of swollen spheres in the solution,  $\Phi$ , calculated according to  $\Phi = cQ\rho_s/\rho_p$ , where  $Q$  is the swelling ratio,  $\rho_s$  the density of the solvent ( $0.95 \text{ g cm}^{-3}$ ) and  $\rho_p$  the density of the polymer ( $1.05 \text{ g cm}^{-3}$ ). All measurements were carried out at  $25^\circ\text{C}$ .

### Pulsed field gradient n.m.r. experiments

With p.f.g. n.m.r. the self-correlation function, that is the (averaged) propagator of the proton ensemble in the system under investigation, is monitored<sup>1</sup>. The pulse programme is shown in Figure 1. The damping of the spin echo,  $A/A_0$ , at finite field gradients is measured experimentally. This damping is caused by displacements of the spins within the diffusion time,  $t$ .  $A_0$  is the signal intensity without applied field gradients. The echo attenuation in dependence on  $t$  and  $q$  is given by:

$$\frac{A}{A_0} \equiv S(q, t) = \exp\left(-q^2 \frac{\langle z^2(t) \rangle}{2}\right) \quad (1)$$

Table 1 Characteristic data of the microgels

Microgel	Molar mass	Latex radius (nm)	Hydrodynamic radius, $R$ (nm)	Swelling ratio, $Q^a$	$D_0^b$ ( $\text{m}^2 \text{s}^{-1}$ )
A400	$1.9 \times 10^8$	42	120	24	$4.0 \times 10^{-12}$
A50a	$1.95 \times 10^8$	42	78	6.3	$5.8 \times 10^{-12}$
A13		13	21	4.3	$2.3 \times 10^{-11}$

<sup>a</sup> In toluene or benzene

<sup>b</sup> Estimated from the hydrodynamic radius and solvent viscosity and the averaging characteristics of p.f.g. n.m.r.<sup>20</sup>

At free diffusion we have  $\langle z^2(t) \rangle = 2Dt$ , with  $D$  the self-diffusion coefficient. If the diffusion is restricted or fractal, the mean square displacement of the species has a weaker time dependence:  $\langle z^2 \rangle \sim t^\kappa$  with  $\kappa < 1$ . In the experiment we then determine an apparent time-dependent diffusion coefficient  $D_{\text{app}} \equiv \langle z^2 \rangle / 2t \sim t^{\kappa-1}$ .

In our experiments,  $q$  was varied by changing  $\delta$  at constant  $g$ . In most cases  $g$  was equal to  $14.5 \text{ T m}^{-1}$ , but  $g$  values as large as  $23 \text{ T m}^{-1}$  were also applied. The length of the field gradient pulses, applied in the time distance of 3 ms between the first and second r.f. pulse and the third r.f. pulse and the echo, respectively, was varied between 0 and 2.4 ms. The diffusion time  $t \gg \tau$  is essentially determined by the time between the second and third r.f. pulse. The microgel A50a was measured at the Kazan University with field gradients up to  $50 \text{ T m}^{-1}$  and in the long-time limit ( $t > 100 \text{ ms}$ ).

The maximum spin echo amplitude,  $A_0$ , is controlled by the proton density in the sample (which determines  $A_{00}$ ) and the nuclear magnetic relaxation of the protons, characterized by their nuclear magnetic relaxation times  $T_1$  and  $T_2$ :

$$A_0 = A_{00} \exp\left(-\frac{2\tau}{T_2} - \frac{t}{T_1}\right) \quad (2)$$

In our system the proton density was small. At a swelling ratio  $Q = 24$  of the microgels only 4% of the swollen sphere was occupied by the polymer, and at a volume fraction of the microgel of 0.25 in the solution the mass concentration of polymer was about 1%. This is roughly the lower limit of sensitivity of our spectrometer for these measurements. The situation deteriorates further owing to the fast initial decay of the transverse magnetization. An example of the magnetization decay measured with a Hahn spin echo experiment is shown in Figure 2. In the p.f.g. n.m.r. experiment transverse magnetization relaxation takes place within the time windows of duration  $2\tau$  (see Figure 1) in which the field gradients are applied, and  $\tau$  must be longer than the maximum field gradient pulse duration  $\delta$  of about 2 ms. We have

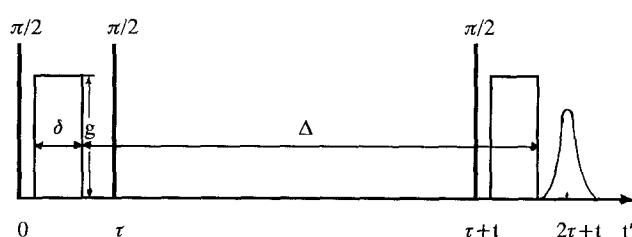
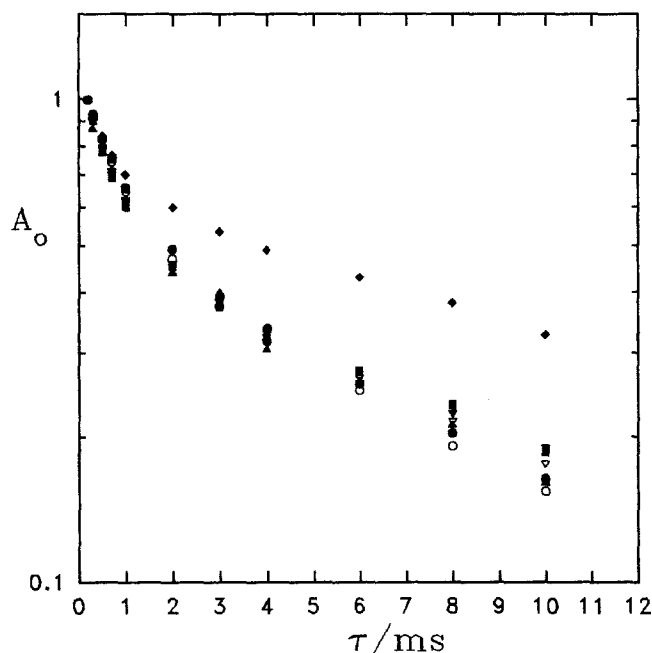


Figure 1 Pulse programme of the stimulated echo experiment in p.f.g. n.m.r.  $\Delta$  is the distance between the two field gradient pulses. The diffusion time is taken as  $t$  for  $\tau \ll \Delta$



**Figure 2** Transverse magnetization decay  $M_{\perp}$  of the protons of the microgel A400 measured with the Hahn spin echo experiment.  $A_0$  is the amplitude of the spin echo in arbitrary units,  $\tau$  is the time between the first ( $\pi/2$ ) and second ( $\pi$ ) r.f. pulse. The concentrations, in mass percentage in the solvent  $C_6D_6$ , are: 1% ( $\blacklozenge$ ), 1.5% ( $\blacktriangle$ ), 2.9% ( $\square$ ), 4% ( $\blacksquare$ ), 5% ( $\nabla$ ), 5.9% ( $\blacktriangledown$ ), 6.9% ( $\bullet$ ) and 7% ( $\circ$ )

chosen  $\tau = 3$  ms. During this time of  $2\tau = 6$  ms about 75% of the magnetization is lost. This fast initial decay of the transverse nuclear magnetic relaxation originates from the 'static part' of the dipole-dipole interaction of protons in the slightly anisotropically moving segments of the network chains<sup>15</sup>. Unfortunately, the rotation of the network spheres is not fast enough for motional averaging of this residual dipole interaction: the rotational correlation time  $\tau_r$  can be estimated to be around 1 ms for the microgel A400 at infinite dilution if the solvent viscosity  $\eta_s$  and the (hydrodynamic) radius  $R$  are placed into the Debye relation  $\tau_r = 4\pi\eta_s R^3/3kT$ . A considerable problem of our measurements is the small signal intensity. Signal accumulation has been shown to be impossible in these experiments since the stability of the large field gradients is insufficient. In this regime a careful equalization of the field gradient pulses by hand is necessary.

In our experiments, we obtained a maximum  $q$  of about  $1.5 \times 10^7 \text{ m}^{-1}$  with  $g_{\text{max}} = 23 \text{ T m}^{-1}$  and  $\delta_{\text{max}} = 2.4$  ms. Thus, the  $qR$  range extends up to  $(qR)_{\text{max}} \approx 1.8$  with the microgel A400 having  $R = 120$  nm (see Table 1). Here the displacements of the protons by rotational diffusion of the spheres should also contribute to the echo attenuation. If we assume that translational and rotational diffusion are independent,  $S(q, t)$  factorizes into a translational part  $S_t(q, t)$  given by equation (1) and a rotational part  $S_r(q, t)$ . If  $\langle z(t)^2 \rangle = 2D_t t$  and  $q^2 R^2 \ll 1$ , with averaging over the volume of the spheres we obtain<sup>16</sup>:

$$S(q, t) = S_t(q, t)S_r(q, t) \\ = \exp(-q^2 D_t t) \left[ 1 - \frac{3}{10} q^2 R^2 + \frac{9}{20} q^2 R^2 \exp(-2D_r t) + \dots \right] \quad (3)$$

where  $D_r$  is the rotational diffusion coefficient and  $R$  is the radius of the swollen sphere. The long-time and small

$q$  limit  $S_r(q, \infty) = 1 - 3q^2 R^2/10$ , which expresses the restriction of rotational motion to the sphere of radius  $R$ , corresponds to the elastic incoherent structure function in quasielastic neutron scattering<sup>3,16</sup>, since it does not depend on the time.  $S_r(q, \infty)$  can, however, decay by translational diffusion over longer distances. For small  $q$ , the time-dependent correction term in equation (3) is dominated by rotational motions if  $q^2 D_t \ll 2D_r$ . If we assume the Stokes-Einstein-Debye relation,  $D_r = 3D_t/4R^2$ , the corrections due to rotation given by equation (3) are rather small for  $q^2 R^2 < 0.5$  and the exact expression for  $S_r(q, t)$  should be used for larger  $q$  values. However, in our microgel solutions it is not clear whether rotation dominates,  $D_r \gg 3D_t/4R^2$ , since translation is largely quenched in densely packed systems, or whether translation dominates since rotation is slowed down by interpenetration in the surface regions of the microgel spheres.

## RESULTS AND DISCUSSION

We have measured  $S(q, t)$  of the microgels as a function of  $q$ ,  $t$  and concentration in solution. Two examples of experimental data are shown in Figures 3 and 4. The curves displaying  $S(q, t)$  versus  $\delta^2 t$  at constant  $t$ , shown in Figure 3 for the large A400 microgel particles, can be related to the question raised above of whether translation or rotation dominates. Since the largest values of  $\delta^2 t$  yield  $q^2 R^2$  between 0.7 and 0.9, equation (3) should be applicable for most of the proton spins. The straight lines of the semilogarithmic plot are in harmony with dominant translational diffusion. Some contribution of rotational motion cannot be ruled out; however, dominant rotation should lead to a larger reduction of  $S(q, t)$  at large  $\delta^2 t$ , as can be inferred from equation (3).

The  $D_t$  values determined from the slopes of Figure 3 decrease with increasing  $t$ . This indicates restricted translational diffusion of the protons, which has also been observed in continuous networks<sup>17</sup> and is discussed further below. That diffusion in our microgel system differs from segmental displacements in continuous networks becomes apparent by comparison with Figure 4,

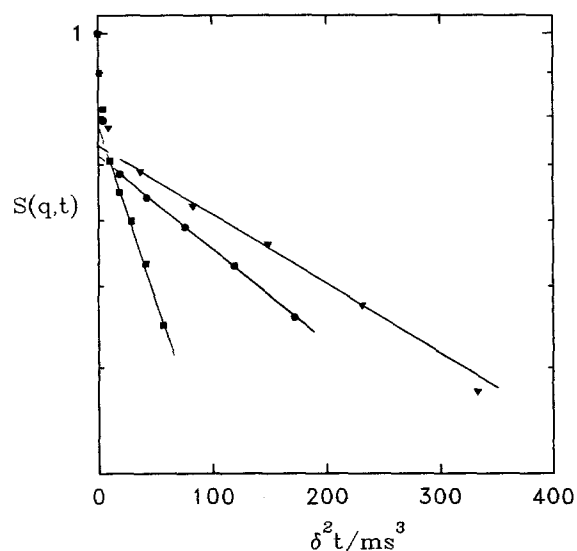


**Figure 3** Echo attenuation of the microgel A400 with concentration of 4% (w/w) ( $\Phi = 0.87$ ) in dependence on  $\delta^2 t$ :  $t = 13$  ms ( $\blacksquare$ ), 53 ms ( $\bullet$ ) and 103 ms ( $\blacktriangledown$ ).  $g = 14.5 \text{ T m}^{-1}$

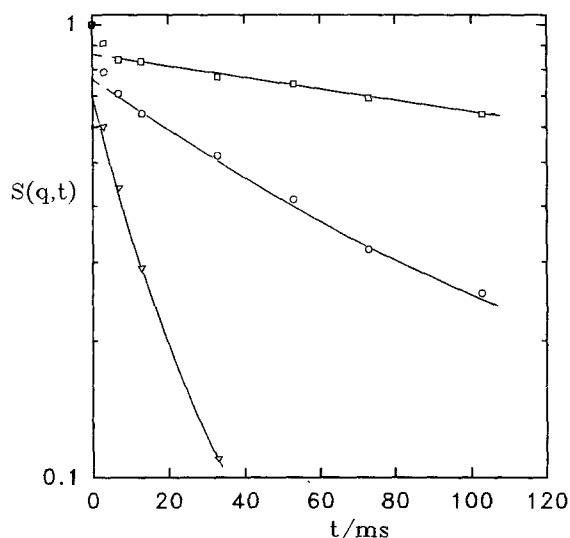


**Figure 4** Echo attenuation of the microgel A13 with a concentration of 19.7% (w/w) ( $\Phi = 0.77$ ) in dependence on time  $t$ :  $q = 4.7 \times 10^{-4} \text{ nm}^{-1}$  ( $\square$ ),  $1.4 \times 10^{-3} \text{ nm}^{-1}$  ( $\circ$ ) and  $2.8 \times 10^{-3} \text{ nm}^{-1}$  ( $\nabla$ )

where the diffusion is faster although the crosslinking density is higher. Here, rotational diffusion can be safely excluded since the maximum  $q$  yields only  $qR \approx 0.06$  for the smaller spheres and  $\log S(q, t)$  versus  $t$  is proportional to  $q^2$ . Figure 4 shows a semilogarithmic plot of  $S(q, t)$  versus  $t$  at different constant  $q$  values. A slowing down of translational diffusion is obtained with increasing diffusion time which is, however, less pronounced than with the larger particles (cf. Figure 7). In Figures 3 and 4, the large apparent volume fractions,  $\Phi = 0.87$  and  $0.77$ , respectively, which are far above the random close packing value of hard spheres, can only be rationalized by deswelling of the network spheres resulting in sphere radii below the dilute solution values of  $R$  listed in Table 1. If we assume some random close packing value,  $\Phi_c$  (e.g.  $\Phi_c = 0.64$  (refs 14, 18)), the corresponding reduced sphere radii for  $\Phi > \Phi_c$  are given by  $R_c = (\Phi_c/\Phi)^{1/3} R$ .

The fast initial decays in Figures 3 and 4 cannot be explained by microgel diffusion since they correspond to apparent diffusion coefficients far above the infinite dilution values  $D_0$  given in Table 1, and considerable proton displacements. We believe that this fast decay must be attributed to traces of emulsifier left over from the synthetic procedures or other low molecular weight impurities.

In Figures 5 and 6 the root mean square displacements, derived according to equation (1), are shown as a function of the microgel concentration in solution. To interpret these results, the Brownian motion timescales of spherical particles in solution are inspected in more detail<sup>19</sup>. Starting at the shortest times, the spheres do not yet feel the neighbouring particles. The fluctuation of the velocity is described with the Langevin equation, and the time constant of this motion is the so-called Brownian time constant  $\tau_B$  which is equal to  $m/f$ , where  $m$  is the mass of the swollen sphere and  $f = kT/D_0$ , the friction coefficient taken at infinite dilution (no hydrodynamic interaction). With the data of Table 1 we obtain  $\tau_B \approx 10^{-8} \text{ s}$ , a time far outside the timescale of our experiment. The time region of the short-time self-diffusion, where no interaction with neighbouring particles is present, ends at the local structure lifetime  $\tau_1$ , a time at which the particles begin to feel the interactions with their

neighbours and collective motion sets in.  $\tau_1$  can be estimated as  $\tau_1 \approx d^2/6D_0$ , with  $d$  the diameter of the particles. Using the data of Table 1 a value of about 2 ms is obtained for the microgel A400, which is about the lower limit of our p.f.g. n.m.r. timescale. In the time region near  $\tau_1$  the particle moves within a 'cage' from which it escapes at times  $t \gg \tau_1$  with the long-time self-diffusion coefficient. This picture is confirmed by our measurements. We see in Figure 5 that at apparent volume fractions  $\Phi$  between about 0.55 and 0.75, the diffusion becomes restricted in our time and space scale:  $\langle z^2 \rangle^{0.5}$  increases only marginally with time. The particles move within a cage, the root mean square displacement of the spins is about 120 nm, which corresponds to the radius of the A400 spheres. At  $t = \tau_1 \approx 2 \text{ ms}$  the root mean square displacement is about 100 nm and roughly independent of concentration. This is the beginning of the long-time self-diffusion out of the cage. Unfortunately, at the high concentrations the long-time limit of

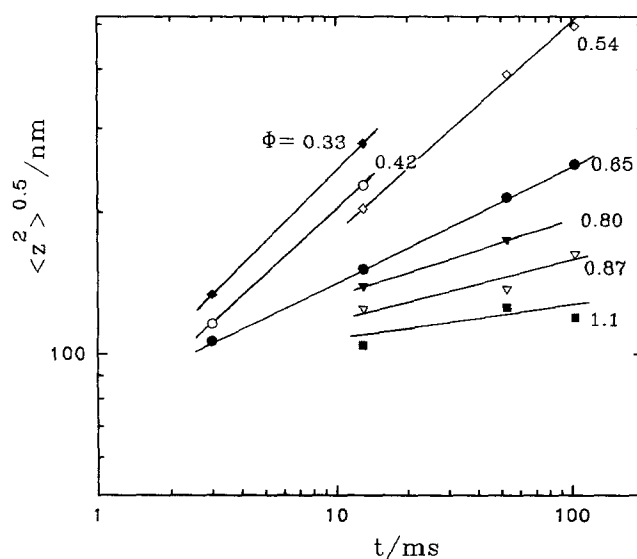


**Figure 5** Root mean square displacement  $\langle z^2 \rangle^{0.5}$  in dependence on the diffusion time  $t$  of microgel A400 for different volume fractions in the solution

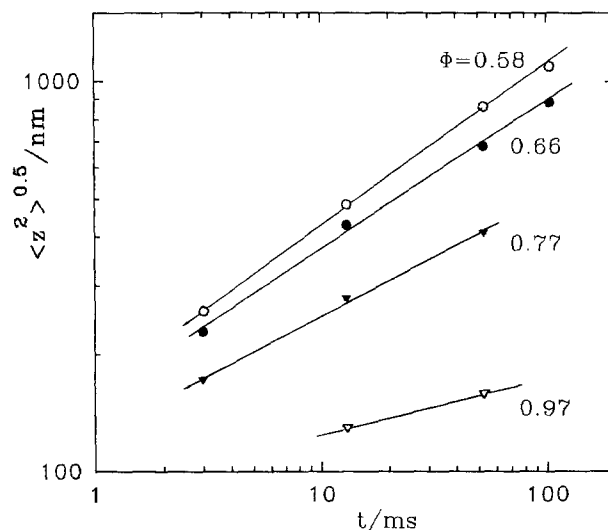


**Figure 6** Root mean square displacement  $\langle z^2 \rangle^{0.5}$  in dependence on the diffusion time  $t$  of microgel A13 for different volume fractions in the solution

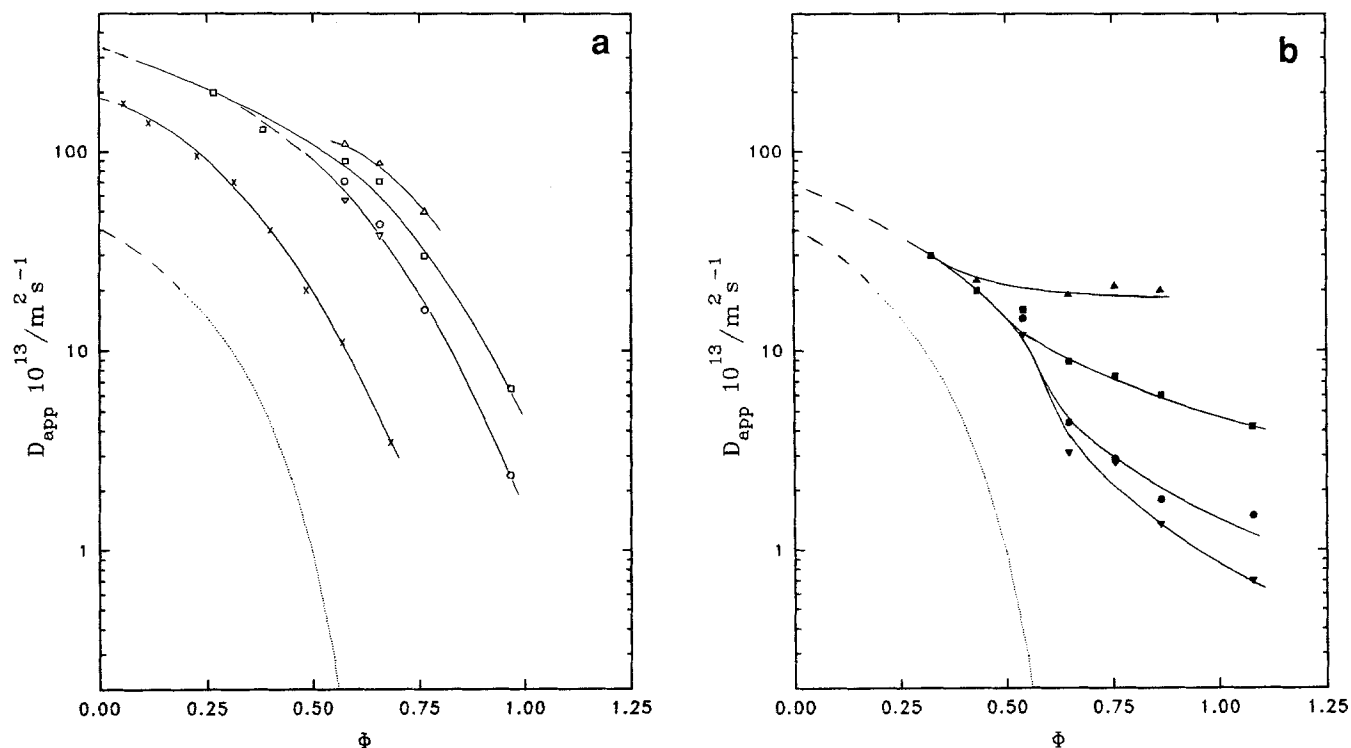


**Figure 7** Apparent diffusion coefficient  $D_{app}$  measured at diffusion times  $t=3$  ms ( $\Delta$ ,  $\blacktriangle$ ), 13 ms ( $\square$ ,  $\blacksquare$ ), 53 ms ( $\circ$ ,  $\bullet$ ) and 103 ms ( $\nabla$ ,  $\blacktriangledown$ ), in dependence on the apparent volume fraction  $\Phi$  of the microgel in the solution. (a) Data for microgel A13 ( $\Delta$ ,  $\square$ ,  $\circ$ ,  $\nabla$ ) and the long-time diffusion coefficient ( $T > 100$  ms) for the microgel A50a ( $\times$ ). (b) Data for the microgel A400. For  $\Phi > \Phi_c = 0.64$  the systems are densely packed with sphere radii reduced by deswelling. The lines are guides for the eye. ---, Long-time  $D_L$  calculated with the Mooney equation (see text) with the parameters  $A=2.72$  and  $k=1.27$  obtained by forced Rayleigh scattering experiments<sup>18</sup> and  $D_0=4.0 \times 10^{-12} \text{ m}^2 \text{ s}^{-1}$

self-diffusion cannot be measured; the timescale is limited due to the nuclear magnetic relaxation of the polymer protons to  $t \lesssim 100$  ms.

In Figure 6, the n.m.r. timescale is well above  $\tau \approx 1.3 \times 10^{-5}$  s and the smallest measured displacements exceed the radii of the A13 gel particles by a factor of about 6. Thus, out of the cage motion of the spheres is observed even at the largest concentrations ( $\Phi=0.97$ ) where the particles are densely packed, and deswelling below the dilute solution value  $Q=4.3$  (Table I) is obvious. Nevertheless, the diffusion slows down with increasing diffusion time, as can be seen most clearly in Figure 7, where the apparent diffusion coefficient  $D_{app} = \langle z(t)^2 \rangle / 2t$  is plotted versus concentration for different diffusion times. Here, the low concentration limit  $D_0$  obtained by extrapolation agrees with the Stokes-Einstein value obtained from solvent viscosity and the radius  $R$  determined by dynamic light scattering. For apparent volume fractions of  $\Phi > 0.6$  we observe time-dependent diffusion coefficients. The slowing down of diffusion with increasing time is most pronounced for the A400 particles where the crosslinking density is low. Here it is possible that a part of the proton displacement is related to sphere deformation. We should also expect cooperative sphere motion leading to slower displacement at longer timescales. In other words, the restricted diffusion of proton spins observed in continuous networks<sup>17</sup> should also be present to some extent in the microgel systems.

In the present n.m.r. experiments the diffusion time is restricted to  $t \leq 100$  ms and any further slowing down over longer timescales cannot be observed. However, further information is obtained from investigations of

photon correlation spectroscopy (p.c.s.) and forced Rayleigh scattering (FRS) in a similar microgel system<sup>14,18</sup>. In the FRS experiments, the incoherent intermediate structure function  $S(q, t)$  is obtained on a timescale  $10 \text{ s} < t < 10^5 \text{ s}$ , far above that of n.m.r. The length scale is also larger than in the n.m.r. experiments and has so far only allowed the monitoring of whole sphere displacements well above  $R$ . In the regime of high concentrations,  $\Phi \approx \Phi_c$ , the decay of  $S(q, t)$  is non-exponential and extends over the whole accessible range of four decades in time. Thus, the slowing down of diffusion for increasing diffusion times, discussed above, in the time domain of  $1 \text{ ms} < t < 100 \text{ ms}$  is continued by a further slowing down detected by FRS. If in these experiments a long-time diffusion coefficient,  $D_L$ , is extracted from the long-time regime of  $S(q, t)$  one can fit the concentration dependence with the Mooney equation,  $\ln(D_L/D_0) = -A\Phi/(1-k\Phi)$ , with the parameters<sup>18</sup>  $A=2.7$  and  $k=1.27$ . This is shown as dashed curves in Figure 7. It represents the lower limit of apparent diffusion coefficients where the largest values are detected by n.m.r. In the p.c.s. experiments, one determines the coherent intermediate structure factor which is related to cooperative (mutual) diffusion. Whereas the length scale is also above that of most n.m.r. experiments in this work, the timescale extends over a very wide range from  $10^{-6}$  to  $10^3$  s (ref. 14). It is difficult to compare the decay in the millisecond regime with the n.m.r. results. However, the interpretation of 'in cage' motions, discussed in relation to Figure 5, corresponds qualitatively to the light scattering results in the same time domain<sup>14</sup>. One can also extract a long-time cooperative diffusion coefficient which can be fitted to the Mooney equation with

parameters  $A$  and  $k$  similar to those of the long-time self-diffusion coefficients.

## CONCLUSIONS

We have measured the incoherent dynamic structure function  $S(q, t)$  of swollen spherical microgels in solution with p.f.g. n.m.r. in the dynamic range from  $qR \ll 1$  up to  $qR \approx 1.8$ . A slowing down of the diffusive motion is observed with increasing volume fraction of spheres in the solution. This slowing down becomes dramatic for  $\Phi \geq 0.6$  and must be attributed to the colloidal glass transition. At these high volume fractions a time-dependent apparent self-diffusion coefficient is observed, more pronounced for the larger of the two microgels where  $qR$  is in the order of 1. The short-time self-diffusion coefficient is interpreted as fast 'in cage' diffusion of the spheres, where contributions by sphere deformation or cooperative sphere motion are also possible. With increasing time the spheres diffuse out of the cage and approach asymptotically the long-range self-diffusion. Rotational diffusion of the spheres should be observable in our experiments with the larger microgel, where  $qR > 1$  is attained, but it was not detected with certainty.

More quantitative information is expected from planned investigations with better characterized microgels free of low molecular traces and with enhanced spectrometer sensitivity. We hope to gain more insight into the rotational and translational dynamics of these systems by increasing the time and concentration ranges investigated and improving the precision of the data.

## ACKNOWLEDGEMENTS

The authors thank A. Doerk and V. Frenz for the preparation and characterization of the polystyrene microgels. G. F. thanks D. Geschke, W. Heink, J. Kärger

and E. Quillfeld for continuous support. Financial support by the Deutsche Forschungsgemeinschaft is gratefully acknowledged.

## REFERENCES

- 1 Kärger, J., Pfeifer, H. and Heink, W. *Adv. Magn. Res.* 1988, **12**, 1
- 2 Callaghan, P. T. 'Principles of Nuclear Magnetic Resonance Microscopy', Clarendon Press, Oxford, 1991
- 3 Fleischer, G. and Fujara, F. in 'NMR—Basic Principles and Progress' (Eds R. Kosfeld and B. Blümich), Vol. 29, Springer, 1993
- 4 Skirda, V. D., Sevrjugin, V. A. and Sundukov, V. I. *Prib. Tekh. Eksp.* 1984, **6**, 122 (in Russian)
- 5 Fleischer, G., Heink, W. and Kärger, J. in preparation
- 6 Callaghan, P. T. and Coy, A. *Phys. Rev. Lett.* 1992, **88**, 3176
- 7 Kimmich, R., Unrath, W., Schnur, G. and Rommel, E. *J. Magn. Res.* 1991, **91**, 136
- 8 Fujara, F., Geil, B., Sillescu, H. and Fleischer, G. *Z. Phys. B. Cond. Matter* 1992, **88**, 195
- 9 Pusey, P. N. in 'Liquids, Freezing and the Glass Transition', Les Houches Session LI (Eds D. Levesque, J.-P. Hansen and J. Zinn-Justin), Elsevier, Amsterdam, 1990
- 10 Schätzel, K. (Ed.) 'Static and Dynamic Light Scattering Techniques and Applications to Dense Colloids', SDLS II meeting, Burg auf Fehmarn, 1–4 March 1993 (abstracts)
- 11 Lilge, D. and Horn, D. *Colloid Polym. Sci.* 1991, **269**, 704
- 12 Antonietti, M., Bremser, W. and Schmidt, W. *Macromolecules* 1990, **23**, 3796
- 13 Antonietti, M., Bremser, W., Müschenborn, D., Rosenauer, Ch., Schupp, B. and Schmidt, M. *Macromolecules* 1991, **24**, 6636
- 14 Bartsch, E., Antonietti, M., Schupp, W. and Sillescu, H. *J. Chem. Phys.* 1992, **97**, 3950
- 15 Geschke, D., Pöschel, K., Doskocilova, D. and Schneider, B. *Acta Polym.* 1985, **36**, 645
- 16 Lechner, R. E. in 'Mass Transport in Solids' (Eds F. Berniere and C. R. A. Catlow), Plenum Press, New York, 1983
- 17 Skirda, V. D., Doroginikij, M. M., Sundukov, V. I., Maklakov, A. I., Fleischer, G., Häusler, K. G. and Straube, E. *Makromol. Chem. Rapid Commun.* 1988, **9**, 603
- 18 Bartsch, E., Frenz, V., Möller, S. and Sillescu, H. *Physica A* in press
- 19 Pusey, P. N. *J. Phys. A* 1975, **8**, 1433
- 20 Fleischer, G. *Polymer* 1985, **26**, 1677